# Lawrence Berkeley National Laboratory

**Title**

Six-Membered-Ring Malonatoborate-Based Lithium Salts as Electrolytes for Lithium Ion Batteries

**Permalink**

https://escholarship.org/uc/item/4833s2nt

**Author**

Yang, Li

**Publication Date**

2012-12-31

# Six-Membered-Ring Malonatoborate-Based Lithium Salts as Electrolytes for Lithium Ion Batteries

Li Yang [a], Hanjun Zhang [a], Peter F. Driscoll [a], Brett Lucht [b] and John B. Kerr [a,*]

[a] Lawrence Berkeley National Laboratory, MS 62-203, One Cyclotron Road, Berkeley, California 94720

[b] Department of Chemistry, University of Rhode Island, Kingston, RI 02881

A new class of lithium salts of malonatoborate anions has been synthesized. These six-membered-ring salts provided slightly lower ionic conductivity than that of LiBOB and $LiBF_4$. Nevertheless, compared with LiBOB and $LiPF_6$, the lowered ring strains in the malonatoborate structures and reduced numbers of fluorine atoms in the molecules was found to enhance the thermal and water stabilities and compatibilities of these salts with ether solvents. Small amount LiDMMDFB when used as an additive, was found to stabilize $LiPF_6$ in carbonate electrolytes at $80^{\circ}C$ for one month. Employing LiMDFB as the electrolyte in Li/Li cells and full cells, large interfacial impedances were observed on lithium metal and the cathode. The large impedances are at least partially attributed to the acidic hydrogen atoms in the malonate structure. This issue can be addressed by replacing the acidic atoms with methyl groups.
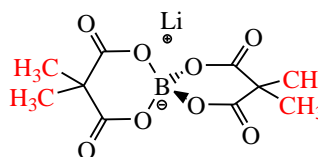
## Introduction
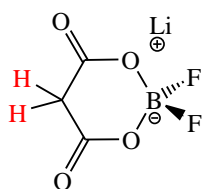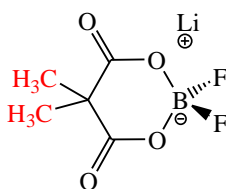


LiMDFB        LiDMMDFB        LiBDMMB

Lithium ion batteries (LIBs) have grown to be one of the most widely used portable power sources[1]. However, loss of power and capacity upon storage or prolonged use especially at elevated temperature ($>50^{\circ}C$) limits the application of LIBs for electric vehicles (EVs) and hybrid electric vehicles (HEVs)[2]. The performance degradation is frequently linked to the thermal instability of $LiPF_6$ and the reactions of the electrolyte with the surface of the electrode materials[3-5]. This has prompted the development of alternative electrolytes for LIBs.

One of the most widely investigated "alternative" classes of salts are oxalate-based

salts such as lithium bisoxalatoborate (LiBOB)[6], lithium oxalatedifluoroborate [LiBF$_2$(C$_2$O$_4$)][7] and lithium tetrafluorooxalatophosphate (LiF$_4$OP)[8] which possess better thermal stability than LiPF$_6$ in both pure salt and electrolyte forms. However, the oxalatoborate electrolytes, possibly due to the high ring strains of their five-membered ring structures, are easily reduced on graphite anode to generate lithium oxalate and borate-rich solid electrolyte interphase (SEI) and appear to contribute to large impedances in the cell. This behavior is implicated in a significant initial irreversible capacity loss which is about 20 % larger than that of a cell with LiPF$_6$ electrolyte[9]. Therefore, the oxalatoborate lithium salts cannot be used as the sole salt in an electrolyte and their application as an additive, especially for LiBOB, has been investigated extensively. However, despite that fact that a small quantity of LiBOB (1%) benefits the cycling performance of LIBs especially at high temperatures, the resulting initial irreversible capacity loss is still at least 10% larger than the standard electrolyte without an additive[10]. Furthermore, oxalatoborate lithium salts are highly sensitive to moisture and can be decomposed in seconds when contacted with water[11].

In this study, a novel family of malonatoborate-based lithium salts have been synthesized and evaluated their chemical and electrochemical performance; in addition, theoretical calculations regarding ring strain energies have been conducted. Although the malonate-based salts have been studied before[12, 13], the comparison between malonate and acidic proton substituted malonate salts has not yet reported.   Comparisons between malonate, oxlate and LiPF$_6$ electrolytes are also presented in this work.


## Experimental

Lithium malonatodifluoroborate (LiMDFB), lithium dimethyl malonatodifluoroborate (LiDMMDFB) and lithium bis(dimethylmalonate)borate (LiBDMMB) were synthesized by reacting lithium malonate and lithium dimethyl malonate with boron trifluoride-etherate (BF$_3$-DEE), followed by recrystalization from ethyl acetate and toluene. Lithium bis-(oxalato) borate (LiBOB) was a gift from Chemetal, Germany and used without further purification. Lithium tetrafluoroborate (LiBF$_4$) was purchased from Sigma Aldrich and used without further purification. The 1M LiPF$_6$-1EC:2DMC electrolyte was a gift from Novolyte, Inc.

Fourier Transform Infrared-Attenuated Total Reflectance (FTIR-ATR) measurements of lithium salts were obtained on a Thermo Nicolet iS10 IR spectrometer equipped with a smart performer accessory with a Germanium crystal. For each sample, 128 scans were collected and purged with high purity argon during entire experiment. The $^1$H, $^{13}$C, $^{11}$B, $^{19}$F and $^{31}$P NMR data were collected on liquid samples with a Bruker 500 MHz NMR spectrometer; the spectra were acquired either in 3EC:7EMC solvent or in D$_2$O. $^1$H and $^{13}$C NMR resonances were referenced to TMS at 0 ppm, $^{11}$B NMR resonances were

referenced to $BF_3 \cdot O(C_2H_5)$ at 0 ppm. ^{19}F and ^{31}P NMR resonances were referenced to $LiP\underline{F}_6$ at -74.5 ppm and $Li\underline{P}F_6$ at -145 ppm, respectively.

LiMDFB: ^{1}H NMR (Acetonitrile-d3, ppm) 3.3 (s), ^{13}C NMR 38, 169, ^{11}B NMR 1.25, ^{19}F NMR -149.4, purity 99.5% with 0.5% $LiBF_4$. LiDMMDFB: ^{1}H NMR (Acetonitrile-d3, ppm) 1.45 (s), ^{13}C NMR 24, 46, 174, ^{11}B NMR 0.33, ^{19}F NMR -147, purity 99.0% with 0.5% LiBDMMB and 0.5% $LiBF_4$. LiBDMMB: ^{1}H NMR (Acetonitrile-d3, ppm) 1.4 (s), ^{13}C NMR 25, 47, 175, ^{11}B NMR 1.7, purity 90% with 9.5% LiDMMDFB and 0.5% $LiBF_4$.

GC-MS analyses were obtained on an Agilent Technologies 6890 GC with a 5973 Mass Selective Detector and a HP-5MS Column. Helium was used as the carrier gas with a flow rate of 3.3 mL/min. Samples were ramped from 30°C to 250°C at 10°C/min. The TGA data were collected on a Perkin-Elmer-7 TGA Instrument by ramping the temperature from room temperature to 600°C at 10°C/min. The electrochemical anodic stability of the electrolyte was assessed by holding the Li/electrolyte/Al cell at each designated voltage (3.5 V, 4.0 V, 4.5 V, 5.0 V, 5.5 V and 6.0 V, respectively) for around 1 hour and recording the current with time.

The conductivities of the electrolytes were measured using a self made, two platinum electrodes cell, calibrated by standard conductivity solutions (1mS $cm^{-1}$ and 10 mS $cm^{-1}$) at varied temperatures, -20 °C, 0 °C, 20 °C, 40 °C and 60 °C. Li/liquid electrolyte/Li symmetric coin cells and Li/Polymer electrolyte/Li symmetric Swagelok cells were fabricated for interfacial behavior studies of the different salts. For liquid electrolytes, the salt concentrations in 3EC:7EMC (v:v) were 1.0 M except for the LiMDFB (0.9M). For polymer electrolytes, lithium salts were dissolved in PEO (Mw 200,000) with a O:Li ratio of 15:1. $LiCoO_2$/electrolyte/MCMB 3032 coin cells were activated by 1 cycle at 1/20 C and 2 cycles at 1/10 C, and cycled ~50 times at 1/5 C. Electrochemical impedance spectroscopy (EIS) analyses of the coin cells were performed using a Solartron 1260 FRA, sweeping from 100 KHz to 0.1 Hz with an AC perturbation amplitude of 10 mV. Quantum mechanics calculations were performed with the free Firefly QC package[14], which is partially based on the GAMESS (US)[15] source code. The details are further explained below.

### Results and discussion

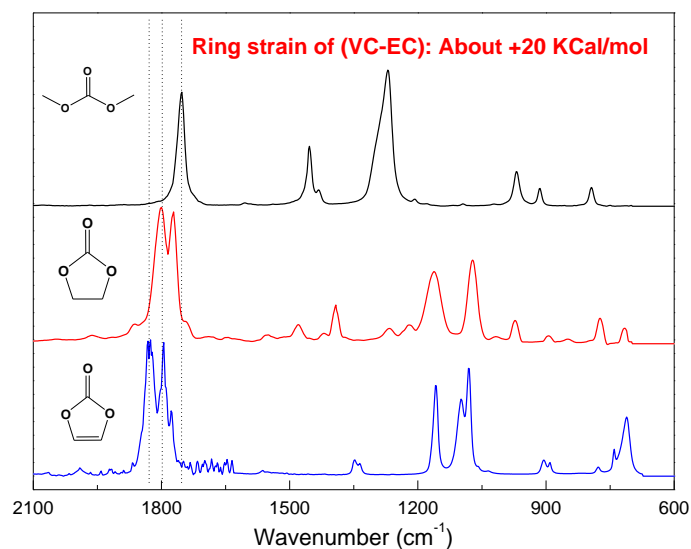### Ring strain of ring structured carbonates and lithium salts

Figure 1. FTIR spectra of DMC, EC and VC

Figure 1 displays the FTIR spectra of pure DMC, EC and VC. It can be seen that as the ring strain increases, the C=O stretching increases to higher wavenumber, from 1750 cm$^{-1}$ to 1800 cm$^{-1}$ and 1830 cm$^{-1}$, for DMC, EC and VC, respectively.
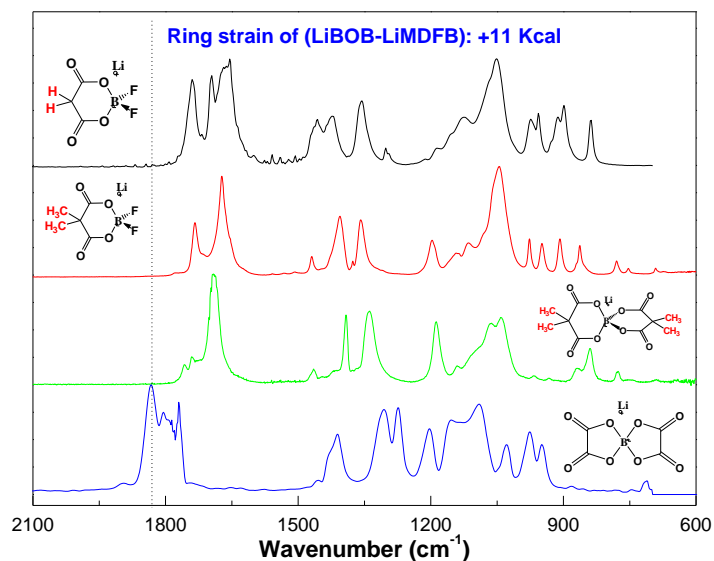


Figure 2. FTIR spectra of the five and six-membered ring salts

Figure 2 shows the FTIR spectra of the Borate salts. Usually the six-membered ring structure possesses less ring strain than five-membered ring structure[16] and Figure 2 showed the same trend as Figure 1. Compared to the oxalate based lithium salts (LiBOB and LiBF$_2$(C$_2$O$_4$)), the malonate based, six-membered ring salts has less ring strain as is evident from the shift in the C=O stretching frequency in Figure 2.
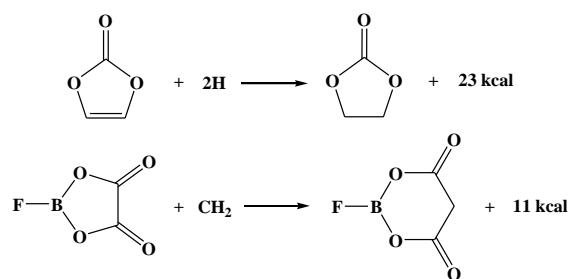
Scheme 1. The relative ring strain of the selected chemical

In order to quantify the relative ring strain of the selected chemical structure, quantum mechanics calculations were performed using previously developed methods[16]. Geometries of all of the molecules selected in this study were fully optimized by using Density functional theory (DFT) and B3LYP method, with 6-31+G (d) basis set. MP2 method with 6-31+G (d) basis set was used for energy calculation based on the optimized geometries. As shown in scheme 1, 23 kcal and 11 kcal relative ring strain for the VC-EC and oxalate-malonate based structure, respectively. Similar calculation methods and basic sets are applied in the calculations detailed below.

## Water stability of the lithium salts

Water stability of the different lithium salts was checked by NMR, as displayed in figure 3. Clearly the LiBOB shows significant sensitivity to $H_2O$ and totally decomposed to form $B(OH)_3$ and $B(OH)_4^-$ in several hours. Nevertheless, LiMDFB appears to be stable in water for days and this advantage over LiBOB is possibly from the lower ring strain of the six-membered ring.
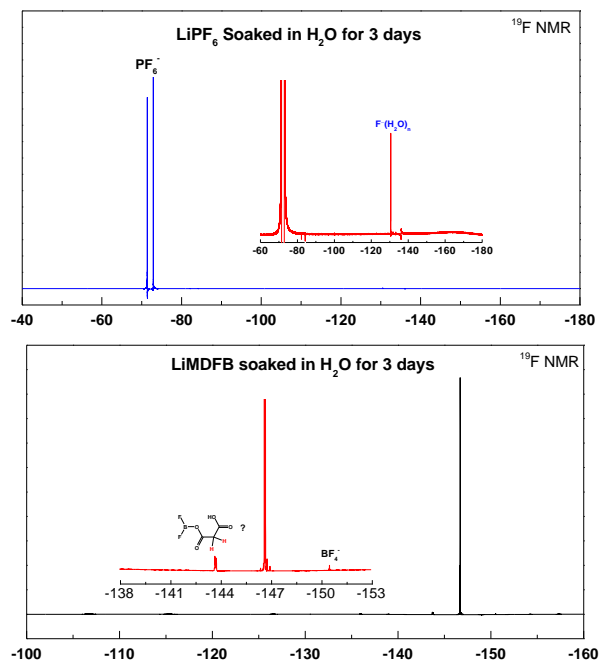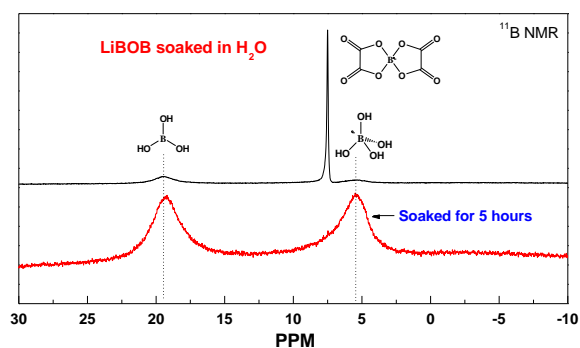
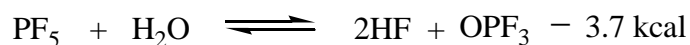Figure 3. $^{19}F$, $^{11}B$ NMR of the lithium salts soaked in $D_2O$

Surprisingly, $LiPF_6$ is quite stable in pure water. It is well known that $LiPF_6$ can be decomposed to form $PF_5$ and LiF (Scheme 2)[3]. In the $LiPF_6$-carbonate based electrolyte, the generated LiF has the least solubility in carbonates and precipitates out from the electrolyte (especially at the electrolyte/graphite interphase) which drives the reaction to the right. With the case in pure water, LiF has much better solubility and hence is much more available for the reverse reaction than in carbonates.
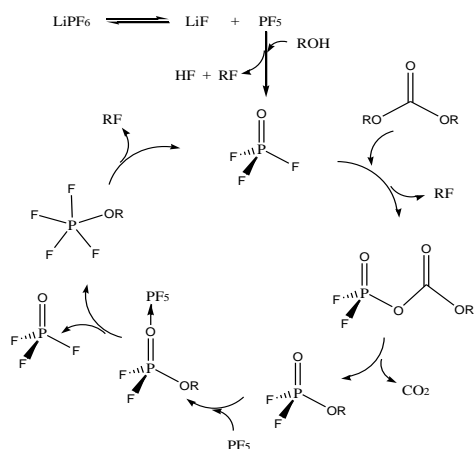
$$LiPF_6 \rightleftharpoons PF_5 + LiF$$
$$+$$
$$H_2O$$
$$\Updownarrow$$
$$2HF + OPF_3$$
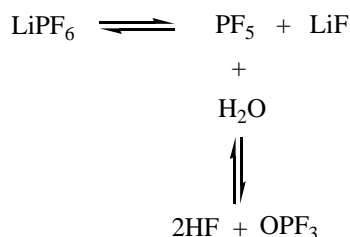
Scheme 2. Decomposition route of $LiPF_6$

Furthermore, the reaction of $PF_5$ with $H_2O$ to form $OPF_3$ and HF is slightly endothermic, $\Delta H = 3.7 kcal/mol$ (scheme 3), based on the quantum mechanics calculation. This does not mean the reaction cannot proceed, if considering the entropy and solvation effect which finally determines the free energy of the reaction. However, this reaction is usually undetectable because of the kinetically dominating $PF_5+LiF \rightarrow LiPF_6$ reaction.

However, in $LiPF_6$-carbonates system, the generated $OPF_3$ by $PF_5$ reacting with trace water can attack other carbonates such as EC and DMC and trigger the autocatalytic decomposition circle (scheme 4), as previously proposed[3], and this drives the decomposition of $LiPF_6$.

$$PF_5 + H_2O \rightleftharpoons 2HF + OPF_3 - 3.7 \text{ kcal}$$

Scheme 3. Reaction enthalpy of $PF_5$ with $H_2O$

LiPF$_6$ $\rightleftharpoons$ LiF + PF$_5$

ROH

HF + RF

RF

RO—C(=O)—OR

RF

F—P(=O)(F)—OR

F$_3$P(F)$_2$—OR

PF$_5$

F—P(=O)(F)$_2$

F—P(=O)(F)—OR

PF$_5$

F—P(=O)(F)—O—C(=O)—OR

CO$_2$

Scheme 4. Autocatalytic decomposition of LiPF$_6$-carbonates

## Compatibility of the salts with PEGDME

**GC data of salts dissolved in PEGDME for 1 week**
— Pure PEGDME 250
— 0.3M LiMDFB-PEGDME
— 0.3M LiBF$_4$-PEGDME
— 0.3M LiBOB-PEGDME

**Decomposition**

0    5    10    15    20    25    30    35
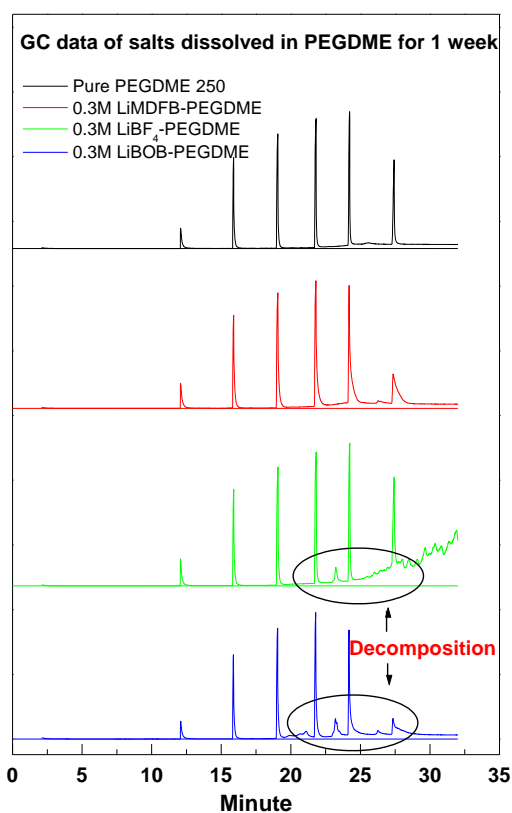**Minute**

Figure 4.    GC analysis of the lithium salts stored in PEGDME 250 for 1 week

The C-O bond in ether is known easily broken by Lewis acid[17]. Figure 4 demonstrates that C-O in PEGDME 250 can be easily broken by LiBF$_4$ and LiBOB, due to the Lewis acid character of the salts. The PEGDME-LiMDFB based electrolyte showed a relatively clean spectrum which implies the weaker Lewis acid behavior of the salt which result from the lower ring strain of malonato based, six-membered ring. Furthermore, it is the higher ring strained, five-membered ring in LiBOB which can

either open under the attack of ethers (SN2 substitution reaction) or transiently open, followed by the attack of ethers (SN1 substitution reaction) that decompose the PEGDME 250, as postulated in scheme 5. Further experiments and theoretical calculations will be conducted to determine the reaction route.



**SN2 Substitution**

**SN1 Substitution**
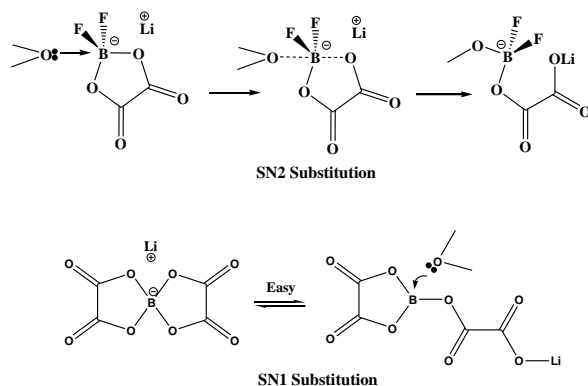
Scheme 5. Possible decomposition mechanism of ether with LiBOB

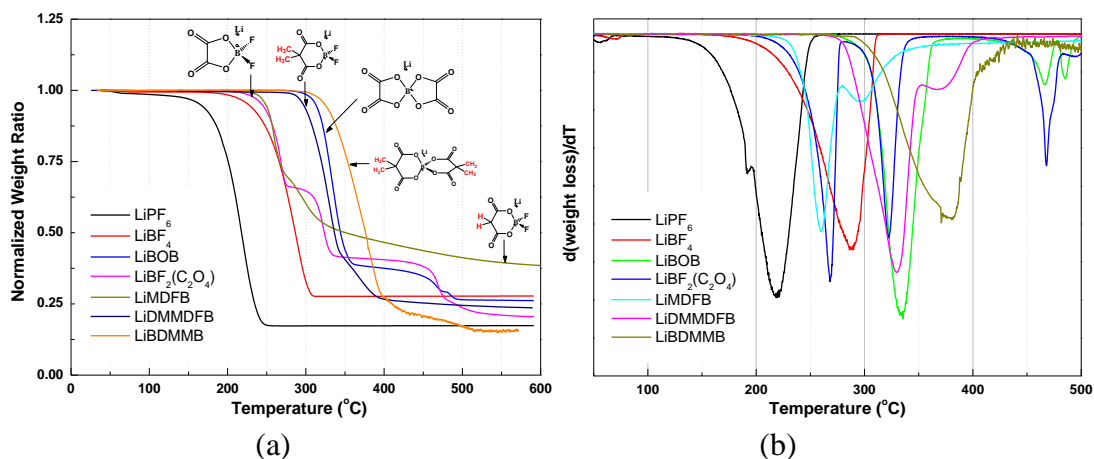**Thermal stability of the different lithium salts**



| (a) | (b) |

Figure 5. TGA of the lithium salts (a), together with the differential data (b).

Table 1. Initial decomposition temperature ($^{o}$C) of lithium salts

| Lithium salts | Initial decompose temperature ($^{o}$C) |
|---|---|
| LiPF$_6$ | 125 |
| LiBF$_4$ | 175 |
| LiBOB | 275 |
| LiBF$_2$(C$_2$O$_4$) | 200 |
| LiMDFB | 220 |
| LiDMMDFB | 270 |
| LiBDMMB | 290 |

From the TGA experiments shown in Figure 5, the LiPF$_6$ and LiBF$_4$ have the lowest

thermal stability and easily form LiF. Comparison of $LiBF_2(C_2O_4)$, LiMDFB and LiDMMDFB shows the initial decomposition temperature increased from 200 $^oC$ to 220 $^oC$ and 270 $^oC$, possibly due to the lower ring strain for the last two salts. The 50$^oC$ difference between the LiMDFB and LiDMMDFB possibly related to the acidic proton in the LiMDFB which tends to release HF at lower temperature. Similarly, the LiBDMMB is slightly thermally stable than LiBOB due to the lower ring strain.

**Electrochemical window of the malonato based lithium salts**
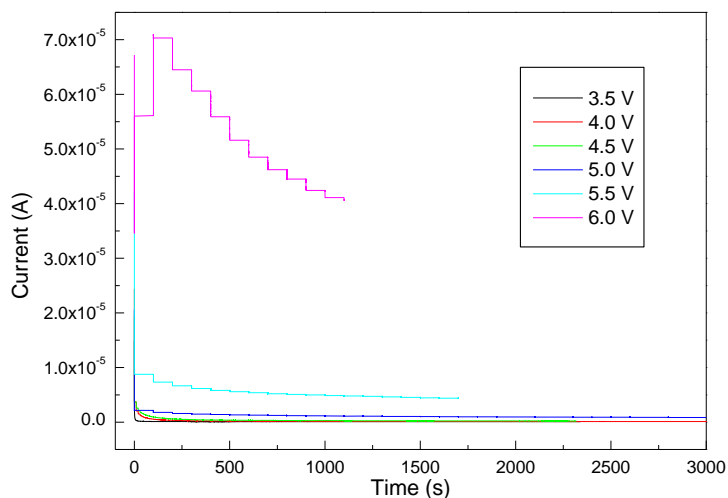


Figure 6. Anodic stability of 0.9 M LiMDFB-3EC:7EMC

The anodic stability of the LiMDFB-EC:EMC is measured by holding the Li/Electrolyte/Al cell at designated voltage (3.5 V, 4.0 V, 4.5 V, 5.0 V, 5.5 V and 6.0 V, respectively where Al is the positive electrode) for 1 hour and the current-time data is recorded, as shown in figure 6. As can be seen the LiMDFB-EC:EMC has a anodic stability up to 5.0 V versus Li/Li$^+$.

Furthermore, in cyclic voltammetry experiments no significant reduction peaks were observed at around 2.0 V vs Li/Li$^+$, which is the typical reduction potential for oxalate salt[9].

**Thermal stability of LiDMMDFB as an additive for 1M LiPF6-1EC:2DMC based electrolyte**
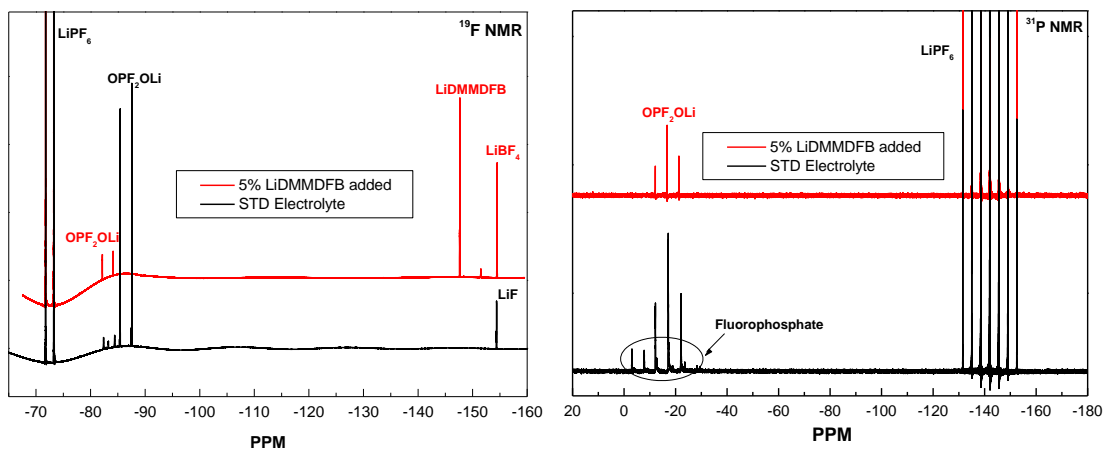
Figure 7. $^{19}$F and $^{31}$P NMR data of the electrolyte with/without LiDMMDFB held at 80$^{o}$C, after 1 month

Thermal abuse of the LiPF$_6$-carbonates based electrolyte with/without LiDMMDFB was conducted by sealing the electrolytes in a flame sealed NMR tube t. The solution of standard electrolyte turned to dark brown in several days under 80 $^{o}$C, while the LiDMMDFB added electrolyte showed no discoloration under 1 month. $^{19}$F and $^{31}$P NMR data (figure 7) showed the LiDMMDFB added electrolyte has relative clean spectra, although some decomposition of LiDMMDFB to LiBF$_4$ was observed. The standard LiPF$_6$-carbonates based electrolyte displayed LiPF$_6$ decomposition to form large amounts of fluorophosphates and LiF[3]. Further thermal abuse experiment of the electrolyte with vials that allow the release of CO$_2$ will be conducted to provide a more realistic test.

### Conductivity of lithium salts in carbonate

The malonate based electrolyte showed a lower conductivity than that of LiBF$_4$ and LiBOB[18] based electrolyte, due to the introduction of an extra –C between the two C=O's. At room temperature, both LiMDFB and LiDMMDFB based salts displayed an ionic conductivity around 1.5 mS/cm (Figure 8) which is still completely satisfactory for most uses.
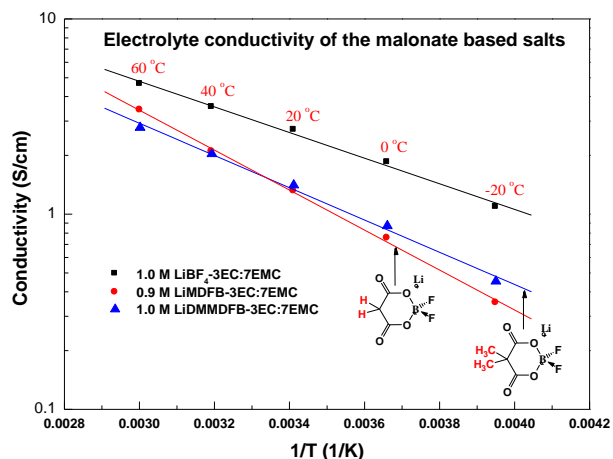
Figure 8.    Conductivity of the different lithium salt in carbonates

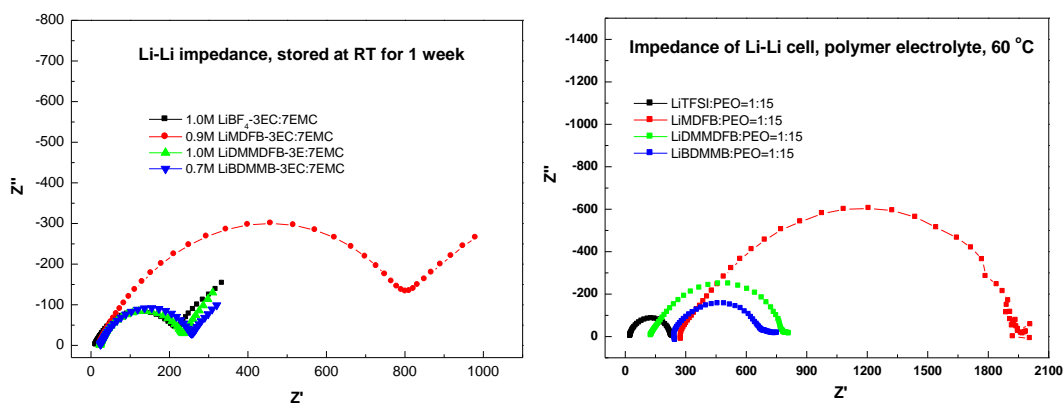## Interfacial behavior of the Li/Li symmetric cell



Figure 9.    Impedance of symmetric Li/Li cell, for liquid electrolyte (left) and polymeric electrolyte (right)

Interfacial behaviors of the different electrolyte system on lithium metal are listed in Figure 9. For Li/Polymer electrolyte/Li Swagelok cells, impedance was measured after the cells were annealed at 80$^{\circ}$C for 12 hours.
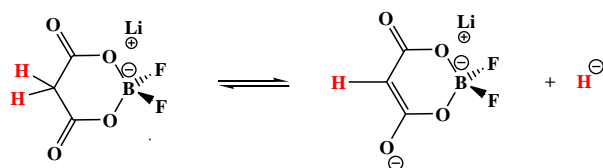


Scheme 6. Acidity Scheme of LiMDFB

As can be seen clearly from both figures that the LiMDFB based electrolyte generates larger interfacial impedance than other salts. This is possible due to the two acidic alpha –H on the molecular (scheme 6). The pKa of the alpha –H in LiMDFB is possible between 7 to 13[19], while for other non-acid H, such as alkanes and THF, the pKa values are ~50.

## Full cell cycling performance of the LiMDFB and LiDMMDFB based electrolyte
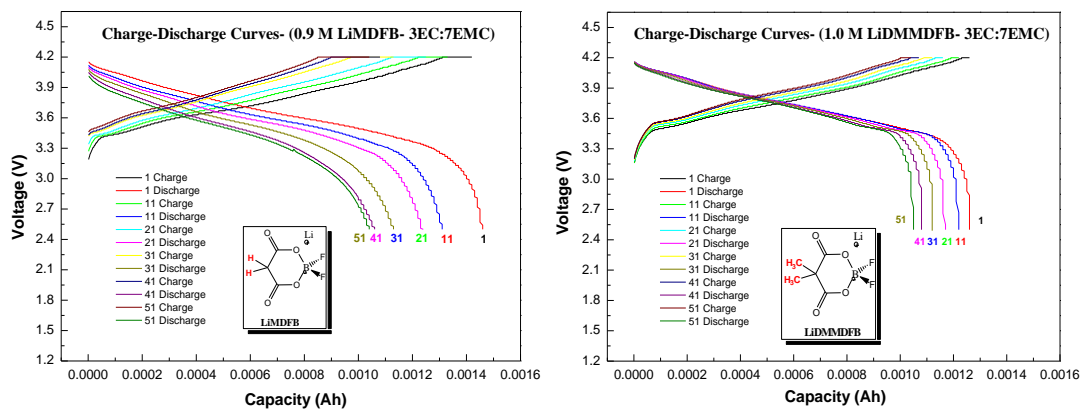
Figure 10.    Charge-discharge cycling profile of LiMDFB and LiDMMDFB based electrolyte

The cycling profile of the LiMDFB and LiDMMDFB based full cell are shown in Figure 10. As can be seen the LiMDFB based full cell showed a faster decrease in both capacity and discharge voltage plateau. The poorer performance possibly resulted from the acidic protons in LiMDFB as mentioned above. AC impedance (figure 11) of the full cells showed the LiMDFB based cell has a much larger interfacial impedance increase after cycling, especially on the cathode side. The cause remains unknown and further study will be needed to elucidate the processes responsible.
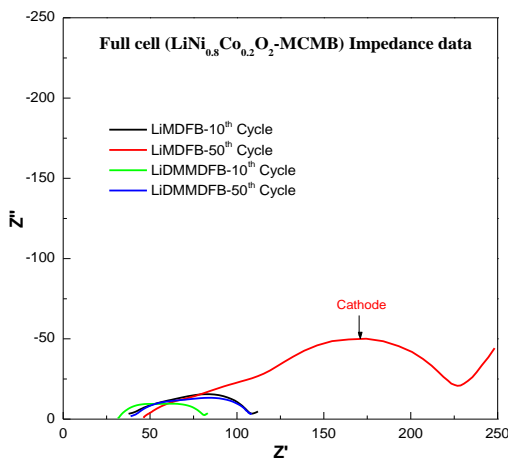


Figure 11. AC impedance of the full cell

## Conclusion

A new class of six-membered ring, malonatoborate based lithium salts showed better thermal stability, water sensitivity and ether compatibility than $LiPF_6$ and LiBOB due to the lower ring strain and fewer fluorides. These lithium salts possess reasonable ionic conductivity at room temperature, although lower than that of $LiBF_4$ and LiBOB. Cycling of Li/Li symmetric cells and $LiCoO_2$/MCMB full cells with the different salts implies that the acidic proton in LiMDFB is the origin of at least part of the high impedance of the

cell. These salts may find their best application as additives for $LiPF_6$-carbonates electrolytes due to their stabilizing effect.

## Acknowledgements

## References

1. *Lithium Ion Batteries: Fundamentals and Performance MWaOY*, Editors, Wiley-VCH, New York (1998).

2. *Diagnostic Examination of Generation 2 Lithium-Ion Cells and Assessment of Performance Degradation Mechanisms.* D. P. Abraham, Editor, Advanced Technology Development Program for Lithium Ion Batteries, U.S. Department of Energy (2005).

3. Campion CL, Li W, Lucht BL. *J.Electrochem. Soc.* 2005; **152**(12): A2327.

4. Li W, Lucht BL. *Electrochem. Solid-State Let.* **10**(4): A115 (2007).

5. Yang L, Ravdel B, Lucht BL. *Electrochem. Solid-State Lett*. **13**(8): A95 (2010).

6. Xu K, Zhang S, Lee U, Allen J, Jow T. *J. Power Sources*. **146**(1-2): 79-85 (2005).

7. Zhang S. *J. Power Sources*. **163**(2): 713-8 (2007).

8. Xiao A, Yang L, Lucht BL. *Electrochem. Solid-State Lett.* **10**(11): A241 (2007).

9. Chen Z, Lu W, Liu J, Amine K. *Electrochim. Acta*. **51**(16): 3322-6 (2006).

10. Santee S, Xiao A, Yang L, Gnanaraj J, Lucht BL. *J. Power Sources*. **194**(2): 1053-60 (2009).

11. Yang L, Furczon MM, Xiao A, Lucht BL, Zhang Z, Abraham DP. *J. Power Sources*. **195**(6): 1698-705 (2010).

12. Xu W, Angell CA. *Electrochem. Solid-State Lett*. **4**(1): E1 (2001).

13. Xu W, Shusterman AJ, Marzke R, Angell CA. *J. Electrochem. Soc.* **151**(4): A632 (2004).

14. Granovsky AA. Firefly version 7.1.G, http://classic.chem.msu.su/gran/firefly/index.html.

15. M.W.Schmidt, K. K. B., J.A.Boatz, S.T.Elbert, M.S.Gordon, J.H.Jensen, S.Koseki, N.Matsunaga, K.A.Nguyen, S.Su, T.L.Windus, M.Dupuis, J.A.Montgomery. *J.Comput.Chem* **14**: 1347 (1993).

16. Dudev T, Lim C. J. Am. Chem. Soc. **120**(18): 4450-8 (1998).

17. Linden, D. I. H. o. B., 2nd ed.; Linden, D., Ed.; McGraw-Hill: New York, Chapters 14 and 36 (1995).

18. Yang L, Smith C, Patrissi C, Schumacher C, Lucht B. *J. Power Sources.* **185**(2): 1359-66 (2008).

19. http://www.chem.wisc.edu/areas/reich/pkatable/index.htm.

## DISCLAIMER

This document was prepared as an account of work sponsored by the United States Government. While this document is believed to contain correct information, neither the United States Government nor any agency thereof, nor the Regents of the University of California, nor any of their employees, makes any warranty, express or implied, or assumes any legal responsibility for the accuracy, completeness, or usefulness of any information, apparatus, product, or process disclosed, or represents that its use would not infringe privately owned rights. Reference herein to any specific commercial product, process, or service by its trade name, trademark, manufacturer, or otherwise, does not necessarily constitute or imply its endorsement, recommendation, or favoring by the United States Government or any agency thereof, or the Regents of the University of California. The views and opinions of authors expressed herein do not necessarily state or reflect those of the United States Government or any agency thereof or the Regents of the University of California.